EXTRACTION OF VEGETATION INFORMATION FOR FORESTRY MANAGEMENTS AND ENVIRONMENTAL MONITORING USING ALOS/AVNIR-2 AND PRISM DATA

PI No. 212

K. Muramatsu[a,b], N. Niino[b], N. Morishita[b], N. Soyama[c], S. Furumi[d], M. Daigo[e]

[a] KYOUSEI Science Center for Life and Nature, Nara Women's Univ., Kita Uoya Nishi Machi, Nara, 630-8506
muramatu@ics.nara-wu.ac.jp

[b] Dept. of Information and Computer Sciences, Nara Women's Univ., Kita Uoya Nishi Machi, Nara, 630-8506

[c] Tenri University, 1050 Somanouchi, Tenri, Nara, Japan,
soyama@sta.tenri-u.ac.jp

[d]Preschool education, Nara Saho College, 806 Rokuyaon-cho, Nara, 630-8565, Japan
sfurumi@nara-saho-c.ac.jp

[e] Faculty of Economics, Doshisha University, Karasuma Higashi-iru Imadegawa-dori Kamigyo-ku, Kyoto, Japan
mdaigo@mail.doshiasha.ac.jp

1 INTRODUCTION

For forestry management and environmental ecological study, vegetation information such as vegetation species and tree heights is important parameters. In japan, forest management information such as the age, height, species and the owner of trees for each area is collected and recorded by the administration of forestry of associations and prefectures. If the trees of one area were cut and the owner would not notify to change the forest management records to the administration office, the records are different from the actual. And the tree heights are estimated using the empirical relationship with the age of trees as a function of the mountain height. The growth of tree is depend on not only the age but also other conditions such as the direction of slope, water conditions, and soil types. Since when the trees are cut for selling, the surveys of diameters measurements at breast heights are needed for all trees and it takes a lot of time, man-power, and costs. If the height of trees and the tree's species can estimate from satellite sensor data, they are useful for forestry managements. Recently, Sato et. al reported the amount of wireworms in the mountain has a relationship with the forest types such as evergreen needle leaf forest and deciduous broad leaf forest. Wireworms control the amount of the land insects in revers. They are important baits for river fishes. Since forest type mapping data is needed from the view points of ecological study. In addition to this, land-cover mapping data with high resolution is needed as validation data sets for low resolution's land-cover mapping results. SGLI sensor on board GCOM-C satellite, which will be launched in 2014, has 250m spatial resolution and it's data will be used for making global land-cover data set.

ALOS satellite was launched in 2006. It has AVNIR-2 and PRISM sensor. AVNIR-2 sensor has four spectral bands 460, 560, 650 and 830 nm with 10 m spatial resolution. PRISM sensor has panchromatic band from 520 nm to 770 nm with 2.5 m spatial resolution and takes data from three directions such as nadir, backward and forward. If use the both of image, pseudo high spatial multi-spectral image can be processed. Because of the spatial resolution and multi-spectral information, these sensor data are expected to useful for making high resolution land-cover data set. In addition to these, PRISM's data from three observation directions is expected to useful to estimate tree heights and to extract vegetation structure information.

We have developed Universal Pattern Decomposition Method (UPDM) (Zhang, L.F. et.al, 2006 (Zhang et al., 2006)) and Modified Vegetation Index based on UPDM (MVIUPD)(Zhang, L.F. et. al, 2007 (Zhang et al., 2007) and Xiong, Y., 2005 (Xiong Yan, 2005)) for satellite sensor data analysis for land cover mapping and vegetation monitoring. In the UPDM method, three coefficients of water, vegetation and soil is calculated using three standard patterns of water, vegetation and soil. One of this method's characteristics is the UPDM coefficients from different sensors for the same object being same as each other. Using this characteristic vegetation cover change was studied with LANDSAT/MSS, TM, ETM+ and ALOS/AVNIR-2 data from 1975 to 2006 (Aoi, M.,et.al, 2006. (Aoi et al., 2006), Aoi, M.,et.al, 2007 (Aoi et al., 2007), Muramatsu, K. et. al, 2008 (Muramatsu et al., 2008)).

In this reports, three analysis results are described. One is vegetation types mapping with ALOS/AVNIR-2 data and UPDM method. Second one is developing the method to calculate the pseudo high resolution data with AVNIR-2 and PRISM nadir observation data to conserve the reflectance. Last one is tree height estimation using PRISM DSM data sets.

2 VEGETATION TYPES MAPPING

From the standpoint of forest management, maps of evergreen forest such as Japanese cedar and cypress and others are needed. From the environmental problem, evergreen forest and deciduous forest data is important and bamboo is spread into "Satoyama" woodland. "Satoyama" woodland means a seminatural area that coexists with a nearby populated area and was important source

of fuel. In this study, vegetation types are set as Japanese cedar, Japanese cypress, deciduous forest, bamboo forest, orchard and grass land.

2.1 Used data

To classify the vegetation types, vegetation phenology is useful. The several data sets observed in the same year should be collected, but the data were limited for sunny days. Although the years are different each other, AVNI-2 data observed on Oct. 9 2006 and Dec. 16 2008 were used.

2.2 Methods

Firstly, characteristics of Universal Pattern Decomposition (UPD) coefficients and Modified Vegetation index based on UPD method (MVIUPD) are studied for each samples. Then classification criteria were determined according to the characteristics. In the following section, Universal Pattern decomposition method (UPDM) and MVIUPD is described briefly.

Universal Pattern Decomposition Method Using the spectral reflectance data, the Universal Pattern Decomposition Method (UPDM) coefficients are calculated. The method is based on the pattern decomposition method (PDM)(Fujiwara 1996, (Fujiwara et al., 1996) Muramatsu 2000 (Muramatsu et al., 2000), Daigo 2004 (**?**)). In the PDM framework, the normalization of standard patterns depends on how many bands and which wavelengths the sensor observes. As the results the obtained patten decomposition coefficients may differ for each sensor such as TM or GLI, even when the same sample is observed. Since the same normalized spectral patterns for any sensor is used in UPDM. In the UPDM, the same value of the coefficients can obtained for results measured by different sensor such as TM or GLI. The method is briefly explained in this section.

The set of spectral reflectance values $(R_1, R_2, \ldots, R_n)$ of n bands for a pixel is transformed into four coefficients such as water (C_w), vegetation (C_v), soil (C_s) with three standard spectral shape patterns. In the three standard spectral shape patterns, three are correspond to typical ground objects, namely water (P_{iw}), vegetation (P_{iv}) and soil (P_{is}). The general equation of universal PDM was as follows:

$$R_i \rightarrow C_w P_{iw} + C_v P_{iv} + C_s P_{is} \ . \tag{1}$$

In UPDM, the standard pattern was defined using the continuous spectral function from 350nm to 2500nm, as follows:

$$\int |P_k(\lambda) d\lambda| = \int d\lambda \ \ (k = w, v, s) \ . \tag{2}$$

Here $\int d\lambda$ refers to integration of the total wavelength range, and $P_k(\lambda)$ is defined as

$$P_k(\lambda) = \frac{\int d\lambda}{\int |R_k(\lambda)| d\lambda} R_k(\lambda) \ \ (k = w, v, s) \ . \tag{3}$$

For each sensor band, the standard patters are defined by

$$P_{ik} = \frac{\int_{\lambda_{si}}^{\lambda_{ei}} P_k(\lambda) d\lambda}{\int_{\lambda_{si}}^{\lambda_{ei}} d\lambda} \ \ (k = w, v, s) \ , \tag{4}$$

where λ_{si} and λ_{ei} are the start and end wavelength for band i, respectively, and $\int_{\lambda_{si}}^{\lambda_{ei}} d\lambda$ is the wavelength with of band i. The decomposition coefficients were obtained for each sensor by the least squares method using the equation 1.

The modified vegetation index based on UPDM was determined as follows:

$$MVIUPD = \frac{(C_v - 0.2C_s - C_4 - C_w)}{C_w + C_v + C_s}. \tag{5}$$

It is determined to have linear relationship with vegetation cover and with the quantity of photosynthesis (XIONG Yan 2005, L.F.Zhang et al., 2004).

2.3 Classification criteria

To select the vegetated area, water and city area characteristics of MVIUPD were studied for summer data. Fig. 1 shows the relationship between MVIUPD and the sum of three coefficients. Water has low values of sum of three coefficients, because water has low reflectance. The values of MVIUPD of city area are less than vegetation area. From this result, water area were determined when the sum of three coefficients are less than 0.04. City and vegetation area were determined when MVIUPD is less than 0.3 and MVIUPD greater than 0.3, respectively.

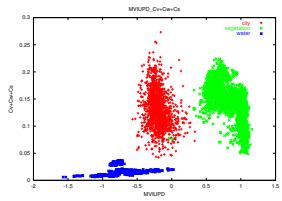

Figure 1: The relationship between MVIUPD and the sum of three coefficients for water, vegetation and city area.

For the vegetated area, the characteristics of UPDM coefficients and MVIUPD values were studied. Fig. 2 (a) and (b) show the relationship between MVIUPD and the sum of three coefficients (SUM), and C_w and C_v of summer data, respectively, for grass with red plots, orchard with pink, bamboo with dark blue , Japanese cypress with blue, and Japanese cedar with yellow. Fig. 3 (a) and (b) show the relationship between C_v and C_s, and C_w and C_s of winter data, respectively, with the same colors plots in Fig. 2. For summer data as shown in Fig. 2 (a), grass and orchard land make clusters, but they are overlapped when the sum of three coefficients is less than 0.18. For winter data as shown in Fig. 3 (a), two clusters of grass and orchard land can be divided with $C_s = 0.08$. In winter, withered grass cause the larger C_s values than orchard land. For bamboo samples, they make a cluster as shown in Fig. 2 (a) and Fig. 3 (a). For Japanese cedar samples,

they make two clusters as shown in Fig. 2 (b). A cluster with higher C_w values correspond to the shaded mountain area and lower C_w values sunny mountain area. Japanese cypress make a large cluster with C_w being less than 0.06.

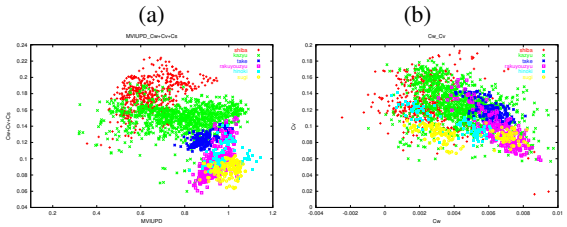

Figure 2: The relationship between (a) MVIUPD and the sum of three coefficients, and (b) C_w and C_v for summer samples of grass with red, orchard with green, bamboo with dark blue, deciduous with pink, Japanese cypress with blue, and Japanese cedar with yellow.

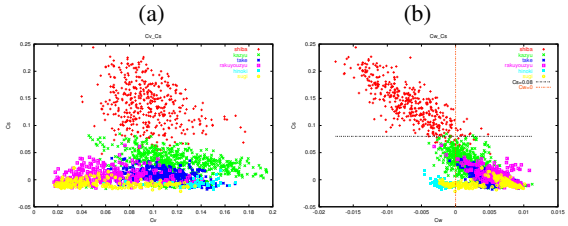

Figure 3: The relationship between (a) C_v and C_s, (b) C_w and C_s for winter samples of grass with red, orchard with green, bamboo with dark blue, deciduous with pink, Japanese cypress with blue, and Japanese cedar with yellow.

Using these characteristics, classification criteria was determined as follows:

(1) Firstly, from the vegetated pixels, grass pixels are selected with the conditions of the sum of three coefficients (SUM) is larger than 0.15 in summer data, and $C_w < 0$ and $C_s > 0.015$ in winter data.

(2) Secondly, from the remainders, orchard land is selected as with the conditions of $SUM > 0.12 MVIUPD = 0.029$ in summer data, and $C_s > 0.01$ in winter data.

(3) Thirdly, from the remainders, bamboo pixels are selected with $SUM > 0.11$ in summer data, and $C_v > 0.08$ and $0 < C_s < 0.015$ in winter data.

(4) Fourthly, from the remainders, Japanese cedar pixels are selected with $C_w < 0.004$ and $C_v < 0.105$, or $C_w > 0.006$ and $C_v < 0.1$ in summer data, and $C_s < 0.01$ in winter data.

(5) Fifthly, from the remainders, Japanese cypress pixels are selected with $C_w < 0.007$ in summer data, and $C_s < 0.01$ in winter data.

(6) Finally, the remainders are classified into Deciduous forest and other vegetation types.

2.4 Vegetation type mapping results

Using these criteria, vegetation types were classified as shown in Fig. 2.4. The classified results are validated qualitatively. The south area of this field has a lot of evergreen forests. The tendency can see from the classified result. In this study, classification category dose not include the paddy area. Since, paddy field is classified into orchard area. In this study, only two seasons data of summer and were used. In spring, paddy field has water. Since if spiring data will be used, the paddy field can be separated from orchard area. Bamboo area was also difficult to classify. The color of bamboo leaf is change to yellow. Since if spring data will be used, the accuracy of bamboo area will be increased. The results should be validated quantitively.

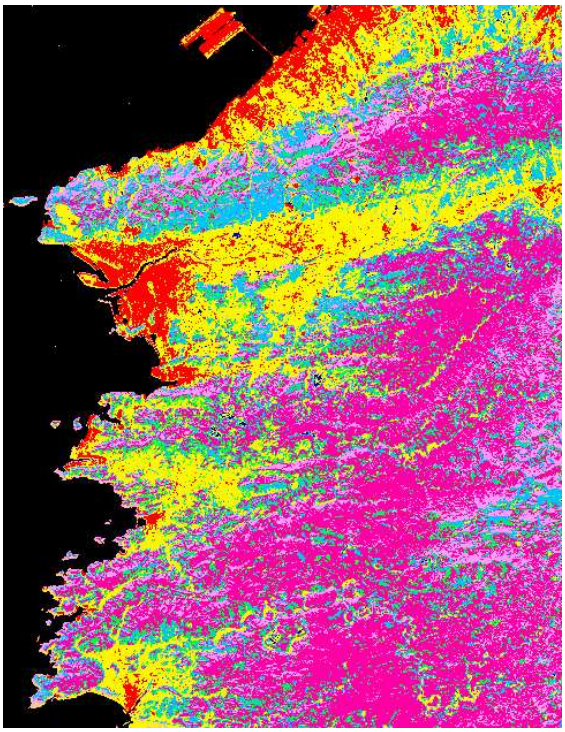

Figure 4: The vegetation types mapping result. Water area are shown with black, city area red, grass dark blue, orchard yellow, bamboo green, Japanese cedar pink, Japanese cypress dark pink, and deciduous light blue. of grass with red, orchard with green, bamboo with dark blue, deciduous with pink, Japanese cypress with blue, and Japanese cedar with yellow.

3 ALGORITHM OF PSEUDO HIGH RESOLUTION MULTI-SPECTRAL REFLECTANCE DATA WITH CONSERVING REFLECTANCE VALUES

3.1 Methods

We used two methods for pseudo high resolution multi-spectral reflectance data making algorithms.

Method 1 is commonly used calculation method using Digital Number for pan-sharping. From the viewpoint of transformation to spectral reflectance, radiance values are used instead of

DN values for the calculation. Visible three bands are commonly used for pan-sharpen processing. The PRISM observation spectral range includes near infrared (Murakami et al., 2009 (Murakami et al., 2009)) as shown in Fig. 5.

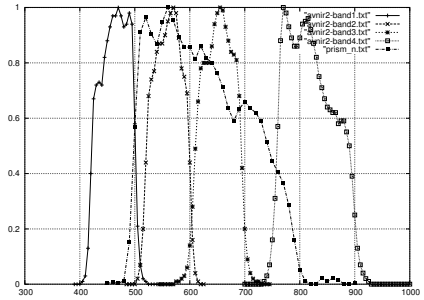

Figure 5: Spectral response curve of PRISM and AVNIR-2.

Since we try to use AVNIR-2 four bands for pan-sharpen processing. The brightness values of PRISM,and band i of AVNIR-2 is described as P and A_i, respectively. The pseudo high resolution brightness values of band i of AVNIR-2 is described as At_i, and it calculates as follows,

$$At_i = nP\frac{A_i}{\sum_{i=1}^{n} A_i}, \tag{6}$$

n : number of bands (3, or 4).

For the processing of pan-sharping, the number of bands are three for color visualization as red, green and blue. PRISM wavelength includes the range of near-infrared. In this study, we use four bands. If four bands can be used, the same criteria can be used for vegetation mapping with AVNIR-2 data sets.

Method 2 is calculation method using spectral reflectance function. The ratio of overlapped area is used for the pan-sharpen radiance calculation. The brightness values of PRISM, and band i of AVNIR-2 is described as P and A_i, respectively. The pseudo high resolution brightness values of band i of AVNIR-2 is described as At_i. The spectral response curve [(**?**)] of PRISM and band i of AVNIR-2 is described as $f_p(\lambda)$ and $f_{a_i}(\lambda)$ as a function of wavelength λ, respectively, and the area (S) inside of the spectral response curve and x axis of PRISM (S_p) and AVNIR-2 (S_{a_i}) is described as

$$S_p = \int f_p(\lambda)d\lambda, \tag{7}$$

$$S_{a_i} = \int f_{a_i}(\lambda)d\lambda. \tag{8}$$

The area inside of spectral response curve of both of PRISM and AVNIR-2 is

$$S_p \cap S_{a_i}. \tag{9}$$

The rate of the overlapped area of Eq. (9) to Eq. (8) is

$$r_i = (S_{a_i} \cap S_p)/S_{a_i}. \tag{10}$$

The rate of overlapped area for each band i of Eq. (9) to Eq. (7) is

$$r_{p_i} = (S_{a_i} \cap S_p)/S_p. \tag{11}$$

The rate of overlapped area for all of bands i of Eq. (9) to Eq. (7) can be described as

$$r_p = \sum_{i=1}^{4}(S_{a_i} \cap S_p)/S_p. \tag{12}$$

Using these equations, the pseudo high resolution multi-spectral brightness can be calculated as

$$At_i = C_i r_p P\frac{r_i A_i}{\sum_{i=1}^{4} r_i A_i}/r_{p_i}, \tag{13}$$

wehere C_i is defined as the correction factor of band i. At the first steps, it is defined as $C_1 = C_2 = C_3 = C_4 = 1$.

3.2 Used data

We used two types of data sets. One is the spectral reflectance and solar irradiance data observed on ground for simulation. Spectral reflectance were measured by FieldSpecFR (ASD. Inc.) for water, vegetation and soil samples and the solar irradiance measured by FieldSpecFR. In order to study the influence of the solar irradiance shape difference, we used the several day's solar irradiance data observed on the rooftop of Nara Women's Univ. by MS-700 (EKO Inc.). We selected the same time and the same day of ALOS observation around Nara area on Aug. 25, Sep. 15, Nov. 10, 2006, Feb. 27, Apr. 5, Apr. 26, 2007. Fig. 3.2 (a) shows the shape of spectral irradiance and the shape of brightness values observed by FieldSpecFR. The solar irradiance shape difference for each observation day are shown in Fig. 3.2 (b). The absorption bands of water vapor around 950 nm is differed each other. But if we focus on the shape, the shapes do not have so large differences.

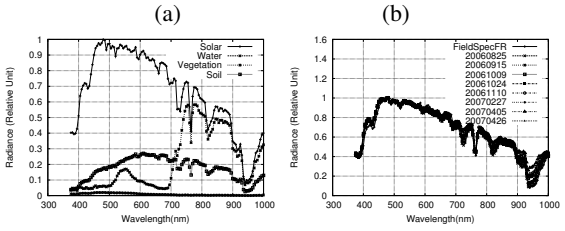

Figure 6: (a) Relative radiance of solar and water, vegetation,and soil samples, and (b)Relative solar radiance observed using MS-700 on ALOS satellite observation dates at 10:30.

Another data sets are AVNIR-2 and PRISM observed on the same day on July 7, 2007 around Miyagawa River in Mie Prefecture.

3.3 Results and discussions

For the ground observation spectral reflectance data sets, the reflectance of before processing and after processing using Eq. (6) and Eq. (13) were compared and the results are shown in Fig. 8 (a) and (b), respectively. In the Fig. 8 (a), the reproductivity of

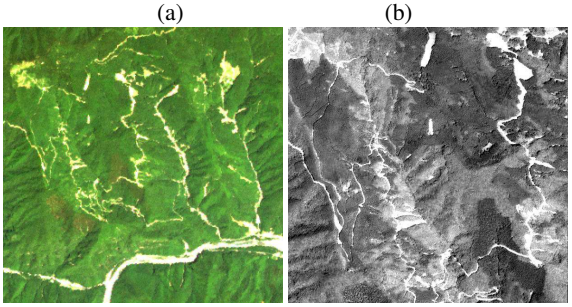

Figure 7: (a) AVNIR-2 image and (b) PRISM image

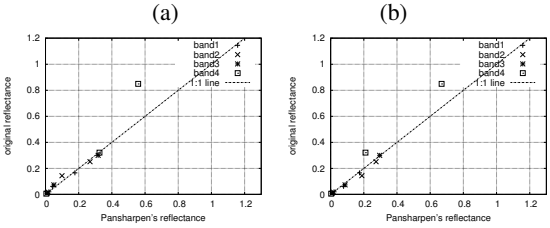

Figure 8: Reflectance of pan-sharpen processing vs. that of original with the Eq. (6). (a) and with the Eq. (13) (b)

reflectance of band 1 to band 3 is good, but band 4 not. In the Fig. 8 (b), the reproductivity of reflectance of band 1 to band 3 is good. For the band 4, both of reflectance values are not on the line 1:1, but all of samples of band 4 are on the same line. It suggests the reflectance difference between before and after processing is systematic, and it is a factor of 1.27. If the correction factor C_4 in Eq. (**??**) is set as 1.27, the reflectance of before and after processing is conserved.

Next, the reflectance reproductivity was studied with AVNIR-2 and PRISM data sets. Fig. 7 (a) show the image of AVNIR-2 and Fig. 7 (b) PRISM of study area. Fig. 9 and Fig. 10 shows the relationship between reflectance values before processing and after processing with Eq. (6) and Eq. (13), respectively. In this case, Rayleigh scattering is subtracted. In Fig. 9, both of reflectance values are on 1:1 line for band 1 to band 3, and are not on for band 4. In Fig. 10, both of reflectance values are almost on 1:1 line for band 1 to band 4. Pan-sharpen image with the mouthed 2 is shown in Fig. 11. From these results, the method 2 has good reflectance reproductivity between befor and after processing.

4 TREE HEIGHT ESTIMATION

4.1 Method and Used data

Using PRISM data observe from different angles, the digital surface model (DSM) can be calculated. Around the mountain area of dense forest, the height of DSM is not ground level, and is the level of forest canopy. If the height of ground level will be subtracted from DSM, tree height can be estimated. The DSM height is defined from the earth ellipsoid. Since the digital terrain model (DTM) data sets are needed to calculate from the height of earth ellipsoid. The DTM is calculated from the height of

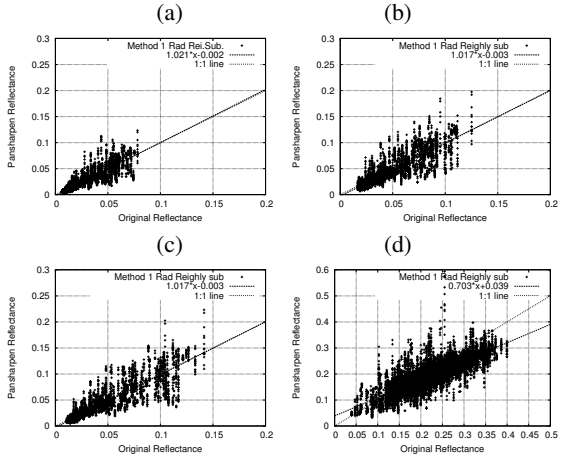

Figure 9: Reflectance of pan-sharpen processing vs. that of original with the Eq. 6 for (a) band 1, (b) band 2, (e) band 3, and (d) band 4.

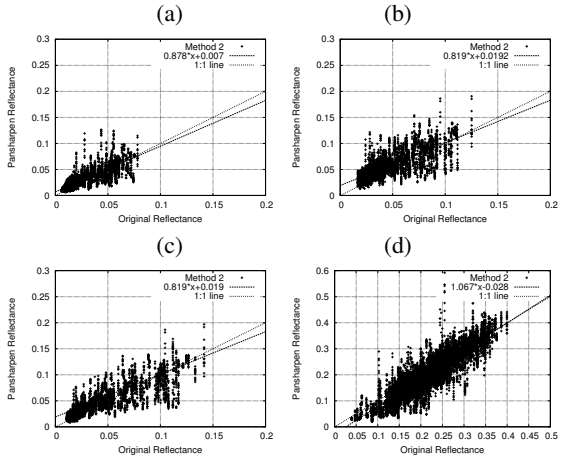

Figure 10: Reflectance of pan-sharpen processing vs. that of original with the Eq. 13 for (a) band 1, (b) band 2, (e) band 3, and (d) band 4.

the geoid and the elevation data sets. These data were download from the homepage of Geospatial Information Authority of Japan, The spatial resolution of the geoid and elevation data is 2 km and 10 m, respectively. Since the data was interpolated with Bi-linear method to set adjust the 2.5 m spatial resolution of PRISM DSM.@In this study, eleven PRISM data sets are used. The observation dates are May 15, June 13, July 18, 2008 and March 18, Sep. 16, Nov. 11, Nov. 18, 2009 and Sep 1, 2010.

For validation, we used two types of data sets. One is forest management records of three villages in Nara Prefecture, and another is radar observation data with helicopter by AERO ASAHI Co.

4.2 Results and discussions

Data sets processing of Nara Prefecture area For making DSM Mosaic data sets in Nara Prefecture, registrations of each image are processed. Using the registration equations of each image, DSM Mosaic data were processed. Fig. 12 shows the Mosaic images of Nara prefecture for (a) PRISM image, (b) DSM

Figure 11: Pan-sharpen image processed with Method 2.

image, and (c) DTM image. To calculate tree height, the absolute height of DTM and DSM are set adjusted each other at the flat area of Nara basin. The tree heights data was processed the height of DTM subtracted from that of DSM as shown in Fig. 12 (d).

Validations Estimated three heights were validated using two types of data sets. Firstly, the estimated values were compared with the radar observation data around Totsukawa village. The data available area is shown in Fig. 13. The DTM and DSM heights were adjusted around river. The ten lines are compared with tree height estimation results. Fig. 14 shows the canopy height, DTM, radar observation data, and the forest management records. We can see the good agreement with each other in Fig. 14 (c), (e), (g), (h). But, at the line 6, estimation tree height were overestimate as shown in Fig. 14 (f). And when the canopy has ruggedness, estimation tree height can not follow the ruggedness and they were flat as shown in Fig. 14 (a), (b) and (d).

Secondly, the estimated values were compared with the tree heigh of forest management records. Fig. 15 shows the histogram of estimated tree heights for each small area of forest managements. The best frequent values of each histogram were compared with the average tree height values in the forest management records. Most of them are agree with each other within the DSM estimation error of $\pm$ 5 m. As shown in Fig. 15 (c), estimation values have minus values. To study the reason, when the tree heights were minus, the area are shown as yellow in Fig. 16. Yellow area corresponds to south slope of the mountain. In this area, the image of back-view has bright values. We consider that difficulty to find the mach pixels between nadir and backward viewing for making DSM causes the large error .

If we will select the area for high accuracy calculation, the tree height estimation data can be used for grasping the situation of tree growth for each mountain area. And if the spatial resolution will be increased in near future, tree height estimation accuracy

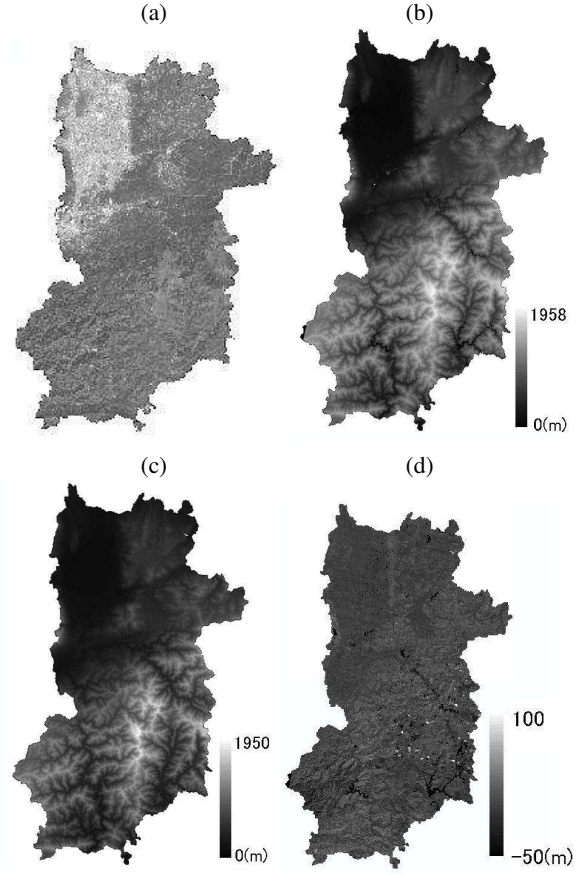

Figure 12: Mosaic images of Nara prefecture (a) PRISM image, (b) DSM image, (c) DTM image, (d) Tree height image.

will become heigh and the data can be used for forest managements.

The Mosaic data sets of DSM, DTM and tree height were submitted to Nara prefecture's administration of forestry with GIS format.These data sets will be given consideration to use the forest management.

5 CONCLUSIONS AND FUTURE WORKS

Firstly, vegetation types can be classified into six categories, such as grass and orchard land, bamboo, Japanese cedar, Japanese cypress, deciduous forest and others. Quantitatively, evergreen forest can be selected, but the classification of cedar and cypress need more validation study. Orchard area includes paddy field and bamboo area was difficult to select. Since if spring data is included for classification, the accuracy will be include. It was difficult to collect winter and summer data of optical sensor data for one year. Next step, seasonal data such as spring, summer and winter will be collected for four or five years and try to make vegetation map.

Secondly, the algorithm of making the data of pseudo high spatial multi-spectral with conserving the original spectral reflectance of AVNIR-2 was developed. If we can collect the data sets of AVNIR-2 and PRISM of nadir observation, the spectral reflectance

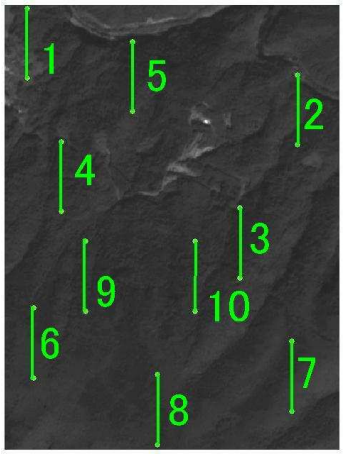

Figure 13: Validation site with LiDAR data

characteristic observed in AVNIR-2 can be used for classification with 2.5 m spatial resolution. This data will be useful for local area study.

Thirdly, tree height was estimated with PRISM/DSM and DTM data calculated from the geoid and elevation data with 10 m spatial resolution. Estimated tree heights were agree with the forest management records and radar observation results except for the area with low DSM estimation accuracy. We consider that the low DSM estimation accuracy was caused to find difficulty of the match pixels between nadir and backward viewing, when when mountain's slope direction is faced with solar light direction and back-viewing sensor catch the brighter reflected light. The Mosaic data sets of DSM, DTM and tree height were submitted to Nara prefecture's administration of forestry with GIS format.These data sets will be given consideration to use the forest management.

ACKNOWLEDGEMENTS

This work was supported by Japan Aerospace Exploration Agency (JAXA) as ALOS project. The data of forest management records was offered by Nara prefecture's administration of forestry. The radar observation data was offered by Nara prefecture's administration of forestry and AERO ASAHI Co. We wishs to express gratitude to Dr. Tadono, Mr. Kageyama, and Mr. Kamimura, Jaxa, for frequent, helpful discussion and supports. We are grateful to Mr. Ueda, Mr. Araki and Mr. Iwai and Ms. Adachi, Nara prefecture forest administration for providing helpful advice and permission to use data. We are grateful to Mr. Ueda, Mr. Araki and Mr. Iwai and Ms. Adachi, Nara prefecture forest administration and Mr. Tanaka and Mr. Umekawa, AERO ASAHI Co. for providing helpful advice and permission to use data.

REFERENCES

Aoi, M., Muramatsu, K., Furumi, S., Daigo, M., Study on land cover classification using universal pattern decomposition method, A study on algorithm for estimation of global terrestrial net primary produuction using satellite sensor data, Doshisha University, World Wide Business Review, Vol. 8, No. 1, 78-92, 2006

Aoi, M., Muramatsu, K., Furumi, S., Daigo, M., Study on applicability to Landsat/MSS of the universal pattern decomposition method, Doshisha University, World Wide Business Review, Vol. 9, No. 1, 137-152, 2007

Daigo,M., A. Ono, R. Urabe, and N. Fujiwara : Pattern decomposition method for hyper-multispectral data analysis, *Int. J. of Remote Sensing*, 25(6), pp.1153–1166, 2004.

Fujiwara,N., K. Muramatsu, S. Awa, T. Hazumi, and F. Ochiai : Pattern expansion method for satellite data analysis (in Japanese), *J. Remote Sens. Soc. Japan*, 16(3), pp.17–34, 1996.

Hill, J., and Sturm, B., Radiometric correction of multitemporal Thematic Mapper data for use *J. Remote Sens. Soc. Japan*, 16(3), pp.17–34, 1996.

Muramatsu, K., Daigo, M., Study on vegetation change in Nara Prefecture for database of environmental change: ALOS/AVNIR-2 data with universal pattern decomposition method, Doshisha University, World Wide Business Review, Vol. 10, No. 1, 161-167, 2008

Muramatsu,K., S. Awa, A. Hayashi, N. Fujiwara, M. Daigo and F. Ochiai : Pattern decomposition method in the albedo space for Landsat/TM and MSS data analysis, *International Journal of Remote Sensing*, 21(1), pp.99–119, 2000.

Hiroshi Murakami, Takeo Tadono, Hiroko Imai, Jaens Nieke, and Masanobu Shimada: Improvement of AVNIR-2 Radiometric Calibration by Comparison of Cross-Calibration and Onboard Lamp Calibration, *IEEE Trans. Geoscience and Remote Sensing*, Vol. 47, No. 12, pp.4051–4059, 2009.

Xiong Yan, A study on algorithm for estimation of global terrestrial net primary produuction using satellite sensor data, *Doctoral thesis, The division of Integrated Sciences, Nara Women's University,* 2005.

Zhang,L.F., S.Furumi, K.Muramatsu, N.Fujiwara, M.Daigo, and L.P.Zhang. : (*International Journal of Remote Sensing*, submitted.) Sensor-independent analysis method for hyper-multi spectra based on the pattern decomposition method, (*International Journal of Remote Sensing*, Vol. 27, 4899-4910, 2006

Zhang,L.F., S.Furumi, K.Muramatsu, N.Fujiwara, M.Daigo, and L.P.Zhang. : Relation between vegetation vigor and new vegetation index based on pattern decomposition method, (*International Journal of Remote Sensing*, Vol. 28, Nos. 1-2, 107-124, 2007

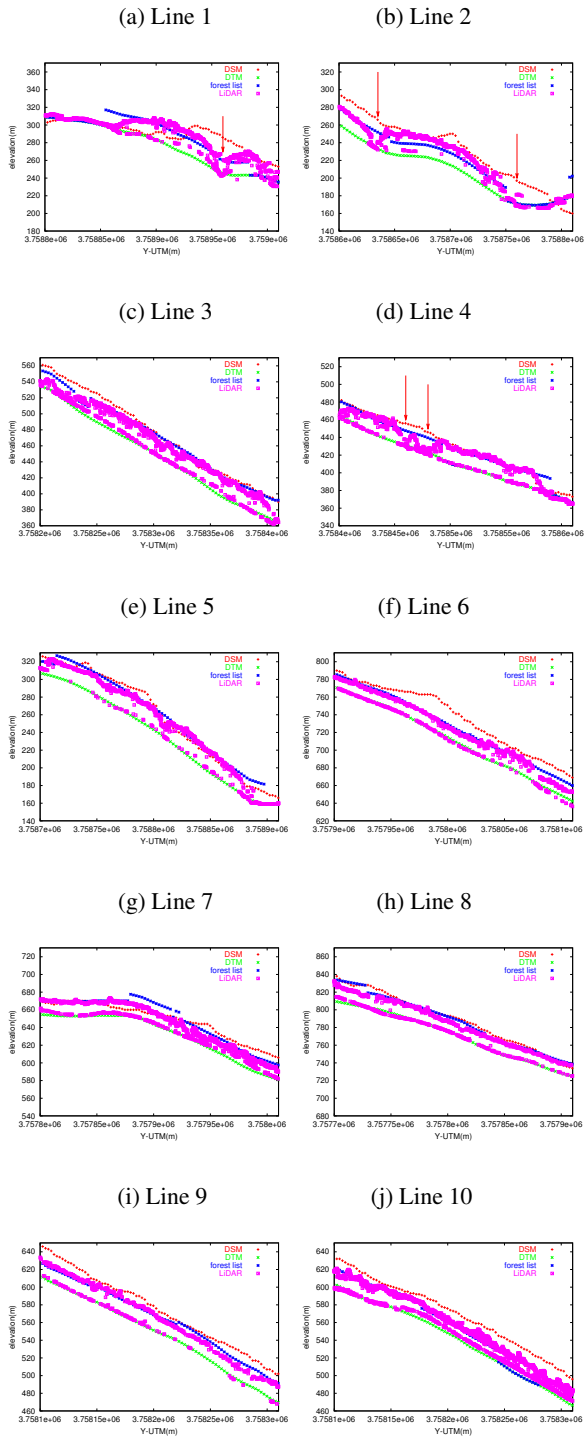

Figure 14: The comparison of DSM, DTM, forest management records, and LiDAR observed eleven lines shown in Fig. 13.

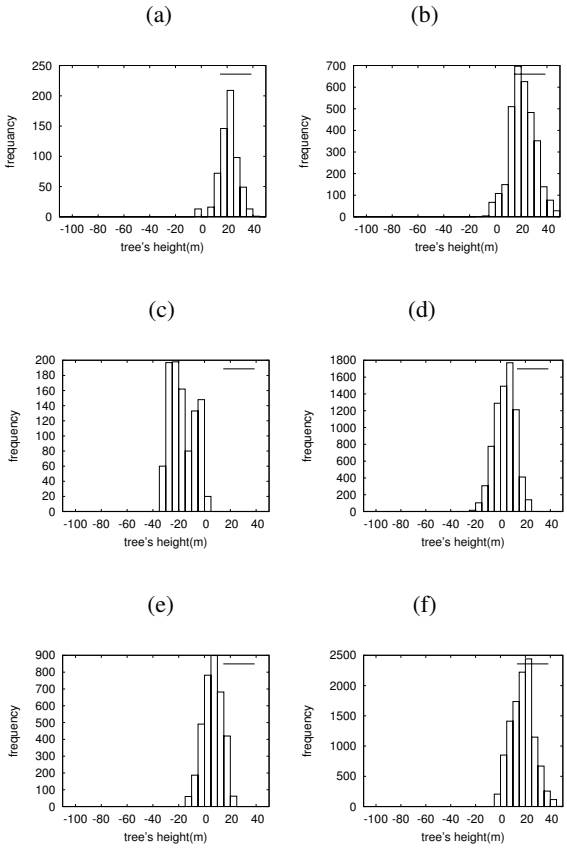

Figure 15: Several examples of tree height histogram estimated using PRISM DSM for each forest management area.

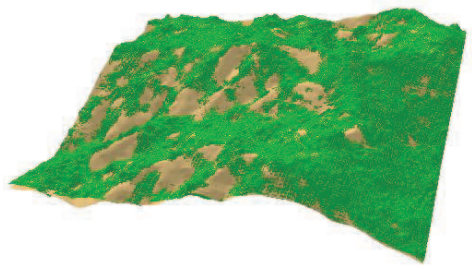

Figure 16: The area of (DSM - DTM) < 0 is shown with yellow around Kawakami village mountain.